Effect of Multiple Alloying Elements on the Glass-Forming Ability, Thermal Stability, and Crystallization Behavior of Zr-Based Alloys

A.I. BAZLOV, A.A. TSARKOV, S.V. KETOV, C. SURYANARAYANA, and D.V. LOUZGUINE-LUZGIN

Effect of multiple alloying elements on the glass-forming ability, thermal stability, and crystallization behavior of Zr-based glass-forming alloys were studied in the present work. We investigated the effect of complete or partial substitution of Ti and Ni with similar early and late transition metals, respectively, on the glass-forming ability and crystallization behavior of the $Zr_{50}Ti_{10}Cu_{20}Ni_{10}Al_{10}$ alloy. Poor correlation was observed between different parameters indicating the glass-forming ability and the critical size of the obtained glassy samples. Importance of the width of the crystallization interval is emphasized. The kinetics of primary crystallization, *i.e.*, the rate of nucleation and rate of growth of the nuclei of primary crystals is very different from that of the eutectic alloys. Thus, it is difficult to estimate the glass-forming ability only on the basis of the empirical parameters not taking into account the crystallization behavior and the crystallization interval.

https://doi.org/10.1007/s11661-017-4441-y

I. INTRODUCTION

METALLIC glasses are non-crystalline materials with a disordered arrangement of the constituent atoms. They possess an interesting combination of high strength, good corrosion resistance, and useful magnetic properties. Metallic glasses (or amorphous solids) were first synthesized in thin-film form by vapor deposition[1,2] and later by rapid solidification from the liquid state at high rates of about 10^5 to 10^6 K/s.[3,4] Subsequently, bulk metallic glasses (BMGs), in large section sizes, were obtained by slow cooling from the liquid state, as in a casting process.[5] BMGs also show a good combination of physical,[5] mechanical,[6–9] magnetic,[10,11] and chemical[12] properties and exhibit high strength, hardness, wear resistance, and large elastic deformation.[13] The largest diameter of the glassy rod with a diameter of 80 mm has been produced in a Pd-based alloy.[14]

The glass-forming ability (GFA) of an alloy is an important parameter that helps in identifying appropriate compositions to achieve glass formation in a wide composition range and also in larger diameters. Several criteria have been proposed to estimate and/or establish GFA of alloys and these are based on either thermodynamic parameters, glass transformation temperatures, or modeling studies. There have been successes with some parameters in some alloy systems and it has been shown that not all the criteria proposed satisfactorily explain the GFA of all alloy systems.[15] Table I lists the different criteria that have been proposed and commonly used in evaluating the GFA of alloys.[16–28]

The GFA of an alloy is determined not only by the composition of the base alloy, purity of the constituent elements, and the atmosphere in which it is cast, but also by the nature of the alloying additions made.[29–31] The atomic size difference between the base metal and the alloying element, their chemical interactions, and thermodynamic properties determine the effectiveness of the alloying element in enhancing the GFA of the alloy system.

Zr-based metallic glasses have been investigated for a long time[32] owing to their good GFA and also their mechanical properties.[33] Starting from thin ribbons obtained by rapid solidification processing,[34] Zr-based alloys have been cast as bulk metallic glasses by slow solidification processes up to about 30 mm in diameter,[35] and currently the maximum diameter reported for a Zr-based glassy alloy is 73 mm.[36] A binary $Zr_{50}Cu_{50}$

A.I. BAZLOV and A.A. TSARKOV are with the National University of Science and Technology MISiS, Moscow, Russia, 119049. Contact e-mail: bazlov@misis.ru. S.V. KETOV is with the Erich Schmid Institute of Materials Science, Austrian Academy of Sciences, 8700 Leoben, Austria. C. SURYANARAYANA is with the Department of Mechanical and Aerospace Engineering, University of Central Florida, Orlando, FL 32816-2450. D.V. LOUZGUINE-LUZGIN is with the WPI Advanced Institute for Materials Research, Tohoku University, Sendai 980-8577, Japan.

Manuscript submitted September 8, 2017.
Article published online December 19, 2017

Table I. Different Criteria Proposed to Understand and Evaluate the GFA of Alloys

Criterion	Formula	References
T_{rg}	$T_{rg} = T_g/T_m$	16
ΔT_x	$\Delta T_x = T_x - T_g$	17
α	$\alpha = T_x/T_l$	18
β	$\beta = (T_x/T_g) + (T_g/T_l) = 1 + \alpha$	18
New β	new $\beta = (T_x \times T_g)/(T_l - T_x)^2$	19
γ	$\gamma = T_x/(T_g + T_l)$	20
γ_m	$\gamma_m = (2T_x - T_g)/T_l$	21
δ	$\delta = T_x/(T_l - T_g)$	22
ω	$\omega = (T_g/T_x) - [2T_g/(T_g + T_l)]$	23
ω_m	$\omega_m = (2T_x - T_g)/(T_l + T_x)$	24
ϕ	$\phi = T_{rg}(\Delta T_x/T_g)^{0.143}$	25
ζ	$\zeta = (T_g/T_l) + (\Delta T_x/T_x)$	26
K_{gl}	$K_{gl} = (T_x - T_g)/(T_m - T_x)$	27
Modified T_{rg}	modified $T_{rg} = (T_e - T_g)/(T_l - T_g)\cdot(T_g/T_l)$	28

Table II. Chemical Compositions (the Subscripts Represent the Atomic Percentage of the Elements) of the Alloys Used in the Present Investigation as Well as from the Literature and Their Thermal Properties (Characteristic Temperatures, T_g Glass Transition Temperature, T_x Crystallization Temperature, T^*_s Approximate Solidus Temperature, T^*_l Approximate Liquidus Temperature, ΔT_x Width of the Supercooled Liquid Region, and ΔT_s the solidification interval) and the Full Width at Half Maximum (FWHM) of the Different Alloys Investigated

Alloy Designation	Alloy Composition	T_g (K)	T_x (K)	T^*_s (K)	T^*_l (K)	ΔT_x (K)	ΔT_s (K)	FWHM (Deg)
ZHE1	$Zr_{50}Ti_{10}Cu_{20}Ni_{10}Al_{10}$ (base alloy)	679	702	1090	1087	23	0	6.1 ± 0.04
ZHE2	$Zr_{50}(Ti,V)_{10}Cu_{20}(Ni,Fe)_{10}Al_{10}$	711	749	1109	1224	38	115	6.59 ± 0.06
ZHE3	$Zr_{50}(Ti,V,Mo,Nb)_{10}Cu_{20}(Ni,Fe)_{10}Al_{10}$	690	749	1105	1140	59	35	5.97 ± 0.06
ZHE4	$Zr_{50}(Ti,V,Mo,Nb,Ta)_{10}Cu_{20}(Ni,Fe,Ag,Co)_{10}Al_{10}$	685	739	1104	1296	54	192	6.03 ± 0.04
ZHE5	$Zr_{50}V_{10}Cu_{20}Ni_{10}Al_{10}$	741	755	1100	1219	14	119	6.52 ± 0.04
ZHE6	$Zr_{50}Ti_{10}Cu_{20}Co_{10}Al_{10}$	669	686	1101	1180	17	79	6.17 ± 0.05
ZHE7	$Zr_{50}Ti_{10}Cu_{20}Fe_{10}Al_{10}$	658	697	1113	1258	39	145	5.8 ± 0.04

alloy (all compositions are given in atomic percent as subscripts) was produced as a BMG with a critical diameter of 2-mm-diameter rod by suction casting.[37] The element Cu was partially replaced by Al to synthesize Zr-Cu-Al glasses with a high GFA and a critical diameter of 8 mm in a $Zr_{50}Cu_{40}Al_{10}$ alloy.[38] Similarly, a hypoeutectic $Zr_{60}Cu_{30}Al_{10}$ BMG alloy showed good GFA[39] and high resistance to fatigue even after complete structural relaxation.[38] By additional alloying with Ni, an element further enhancing the GFA of Zr-Cu-Al alloys,[17] $Zr_{60}Cu_{20}Ni_{10}Al_{10}$ alloy exhibiting a high resistance to structural relaxation-induced embrittlement was produced. The addition of Ti was found to further improve the GFA of these alloys by enhancing the icosahedral short-range order in the $Zr_{62-x}Ti_xCu_{20}Ni_8Al_{10}$ liquid alloys.[40]

During the last decade or so, research on multicomponent alloys has received lot of attention.[41–43] These alloys contain either equiatomic proportions of a large number of elements (5 or more), each with a concentration of 5 to 35 at. pct, or multicomponent alloys with one major element and all the others with equal atomic percentages. Such alloys can be called multiprincipal element alloys but are more commonly referred to as high-entropy alloys (HEAs). Bulk metallic glasses have also been produced in such multicomponent alloys, *e.g.*, $Ti_{20}Zr_{20}Hf_{20}Ni_{20}Cu_{20}$.[44] The process of glass formation, thermal stability, mechanical properties, and corrosion resistance of a number of multicomponent bulk glassy alloys such as $Zr_{55}Al_{10}Fe_6Co_6Ni_6Cu_6Pd_6Ag_5$ have also been studied recently.[45]

In this publication, we report our results on the synthesis, GFA, and crystallization behavior of a number of glassy alloys based on the $Zr_{50}Ti_{10}Cu_{20}Ni_{10}Al_{10}$ alloy. Here, Ti and Ni have been replaced with similar early (V, Mo, Nb, Ta) and late (Fe, Ag, Co) transition metals, respectively. We have also evaluated the GFA of these alloys in terms of the known GFA parameters listed in Table I.

II. EXPERIMENTAL PROCEDURE

The multicomponent alloys with the nominal atomic compositions listed in Table II were chosen for the present study. Master alloys were prepared by melting the mixture of pure metals with purities exceeding 99.9 mass. pct in a Ti-getter argon atmosphere. From these ingots, glassy alloy ribbons of around 20 μm in thickness and 2 mm in width were produced by melt spinning on a single copper roller, while bulk samples were cast into a pyramidal-shape mold having 5 mm base. This helped us in determining the maximum diameter at which glasses have formed by visual observation and later confirmed by X-ray diffraction (XRD) studies.

The structure of the as-solidified and crystalized samples was examined by XRD analysis using a Bruker D8 Advanced diffractometer with Cu Kα radiation. The thermal properties of the glassy alloys were measured using a Setaram Labsys differential scanning calorimetry (DSC) instrument under an Ar gas flow. The samples were also heated to the corresponding crystallization temperatures (T_x) to study the early stages of the crystallization process.

The GFA of the different alloys was also evaluated in terms of the parameters proposed by different authors[16–28] and correlations were made between the alloy characteristics and the GFA parameters.

III. RESULTS AND DISCUSSION

A. *Structure and Transformation Temperatures*

Figure 1(a) presents the XRD patterns, while Table II lists the full width at half maximum (FWHM) and thermal properties of the different multicomponent alloy ribbons studied in this work. All the alloys showed broad and diffuse diffraction peaks, suggesting formation of an amorphous phase. The alloying elements exhibited a strong effect on the FWHM values of the alloys. Analysis of the XRD patterns showed that the FWHM observed was the lowest for the $Zr_{50}Ti_{10}Cu_{20}Fe_{10}Al_{10}$ alloy (ZHE1). While the FWHM for the base amorphous alloy was 6.1 ± 0.04 deg, complete replacement of Ti by V led to a slight increase in the FWHM value. Substitution of nickel by iron and titanium by vanadium increased the FWHM of the alloys by ~ 0.5 degree. Together, addition of V, Ni, Mo, and Nb slightly decreased the FWHM of the alloy. The largest value of 6.59 ± 0.06 deg for the FWHM was observed for the (ZHE2). But, complete replacement of Ni by Fe reduced this value to a minimum level of 5.8 ± 0.04 deg (ZHE7). In other cases, full or partial replacement of elements didn't have high effect. These results allow us to make some guesses about the stability of the amorphous phases.

Figure 1(b) presents a HRTEM image and a diffraction pattern of ZHE3 alloy in the as-cast state. A diffuse diffraction ring can be observed in the diffraction pattern. Also, no crystalline planes are detected in the HRTEM image which indicates formation of the amorphous single phase.

Figure 2 presents a typical DSC trace, while Table II also lists the characteristic temperatures of the different alloy ribbons studied. Analysis of the DSC results showed that the multicomponent alloy $Zr_{50}(Ti,V,Mo,Nb)_{10}Cu_{20}(Ni,Fe)_{10}Al_{10}$ (ZHE3) has the maximum interval of supercooled liquid region (Table II). Full replacement of titanium by vanadium led to a substantial increase in both T_g (from 679 K to 741 K) and T_x (from 702 K to 755 K). On the other hand, partial replacement increased only T_x, but did not change T_g (except for ZHE2), thereby increasing the interval of the supercooled liquid region from 23 K to 59 K. Replacement of nickel by cobalt or iron led to a slight decrease in both T_g and T_x, but a slight increase in T_l. Partial

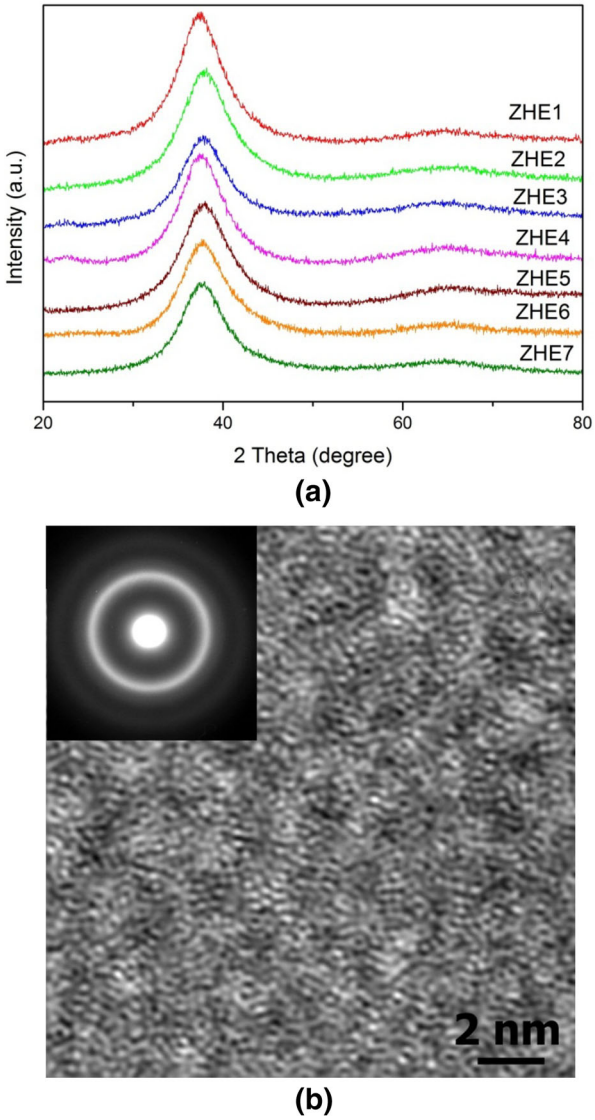

Fig. 1—X-ray diffraction patterns of the as-solidified ribbons (*a*), a HRTEM image (*b*), and diffraction pattern (inset) of ZHE3 alloy.

replacement of titanium and nickel by vanadium and iron, respectively, led to an increase in the interval of the supercooled liquid region. These changes in the characteristic temperatures lead to different GFA values of the alloys, to be described later.

The above results can be rationalized as follows. The thermal stability of the glass and its transformation behavior are determined by the T_g and T_x temperatures. By looking at the effect of the different solute elements on these parameters, described above, it becomes clear that the transformation temperatures are significantly increased when the structure or the atomic size (or both) of the alloying element is significantly different from the element it is replacing. On the other hand, when the structure is similar and the atomic size is also similar, then the alloying element will not have any measurable effect on the transformation temperatures.

Replacement of nickel for iron (ZHE1 and ZHE7 alloys) increases the intervals of the supercooled liquid

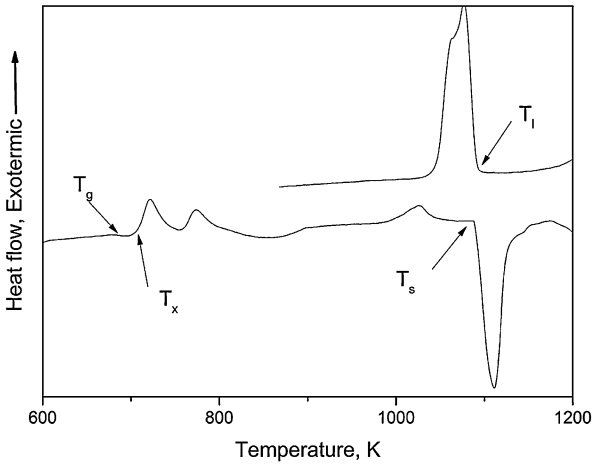

Fig. 2—DSC curve of the ZHE1 alloy.

and the crystallization interval, that is, the thermal stability of the supercooled liquid increases, but at the same time the critical cooling rate necessary for obtaining the amorphous state increases, since we move away from the eutectic point. The replacement of titanium with vanadium (ZHE1 and ZHE5) and nickel by cobalt (ZHE1 and ZHE6) reduces the thermal stability of the supercooled liquid, and also deteriorates formation of the amorphous phase during casting due to the increase in the crystallization interval. Partial replacement of titanium and nickel perfectly stabilizes the supercooled liquid; however, in all alloys except for ZHE3 the crystallization interval increases dramatically, which makes it difficult to obtain BMGs in these alloys.

B. *Crystallization Process*

All the alloys were subjected to a short crystallization treatment of a 10-minute anneal at the crystallization temperature, T_x, and the resulting XRD patterns are presented in Figure 3. The XRD patterns of the alloys with the highest Ti content (ZHE1, ZHE6, and ZHE7) are very similar to the as-solidified alloys, but with minor differences. For example, a trace amount of the ZrO_2 phase is present owing to surface oxidation. Further, the broad maxima are slightly sharper than in the as-solidified condition (Figure 3). The FWHM of the diffraction peaks have decreased to 4.50 (ZHE1), 4.79 (ZHE6), and 5.05 (ZHE7) degrees indicating that nanocrystallization has occurred in these alloys. A similar effect was found earlier in Cu-Zr-Ti alloys. While the primary crystals during crystallization of glassy Cu-Zr alloys are usually large,[46] they are much finer (*i.e.,* nanocrystallization of the primary phase occurs) with the addition of Ti.[47]

All alloys with low titanium content (ZHE2, ZHE3, and ZHE4) exhibit a similar crystallization process. Crystals of Zr_2Cu (I4/mmm) and $ZrAl_3$ ($Fm\bar{3}m$) phases grow from the amorphous matrix at the first stage of crystallization process, likely by a eutectic reaction. In the titanium-free alloy (ZHE5), the crystallization process started with the formation of the Zr_2Ni (I4/mcm) phase. Based on these results, we can say that even though titanium decreases the thermal stability of these alloys (decreasing T_x), it also causes nanocrystallization. Also, despite the fact that the heating of samples was carried out under an argon atmosphere, the surface was oxidized and the ZrO_2 peaks are present in the XRD patterns. Table III shows the crystallization and melting enthalpies of the studied alloys. Correlations between the obtained values are shown in Figure 4.

C. *Glass-Forming Ability*

It was mentioned in the Introduction that a large number of criteria were developed to predict the GFA of alloys. Since the present series of alloys can also be considered multicomponent (high-entropy) alloys, let us first see if the GFA of these alloys can be rationalized in terms of the criteria developed for HEAs.

Majority of the HEAs are expected to form solid solution phases.[41–43] Depending on the atomic size difference, δ, and the thermodynamic properties (entropy of mixing, ΔS_{mix}, and enthalpy of mixing, ΔH_{mix}) of the constituent elements, it was reported[48] that a solid solution phase forms when δ is small and the value of ΔH_{mix} is near zero (not negative enough to form intermetallic compounds). On the other hand, large values of δ and more negative ΔH_{mix} values were noted to promote glass formation. These arguments were further extended by Yang and Zhang,[49] who introduced the Ω parameter to determine if solid solutions form in these multicomponent alloys or not.

Calculation of Ω also makes use of the parameters T_m, the melting temperature of the n-element alloy, ΔS_{mix}, and ΔH_{mix}, and the Ω parameter is defined as

$$\Omega = \frac{T_m \Delta S_{\text{mix}}}{|\Delta H_{\text{mix}}|},$$

where $T_{\text{m}} = \sum_{i=1}^{n} c_{\text{i}} (T_{\text{m}})_{\text{i}}$, where $(T_{\text{m}})_{\text{i}}$ is the melting point of the ith component of the alloy, $\Delta S_{\text{mix}} = -R \sum_{i=1}^{n} (c_{\text{i}} \ln c_{\text{i}})$ is the entropy of mixing of an n-element regular solution, and $\Delta H_{mix} = \sum_{i=1, i \neq j}^{n} \Omega_{ij} c_i c_j$ is the enthalpy of mixing for the multicomponent alloy system with n elements, where $\Omega_{\text{ij}} = 4\Delta H_{\text{AB}}^{\text{mix}}$.

The prediction of a solid solution or a bulk metallic glass was made by considering both the δ and Ω values. It was shown that a solid solution forms if the δ values are small ($\leq$ 6.6 pct) and Ω is $\geq$ 1.1. On the other hand, BMGs are expected to form if the value of δ is larger and the Ω value is smaller. These thermodynamic parameters have been calculated by most authors on the basis of a regular solution model, even though such an assumption was questioned recently.[50]

The results of our calculations of δ and Ω for the different alloys studied are shown in Table IV. A few points are of interest. Firstly, all the alloys have the same δ value, 9.9 pct, which is $>$ 6.6 pct. Secondly, the value of ΔH_{mix} is negative, but quite small. Thirdly, the

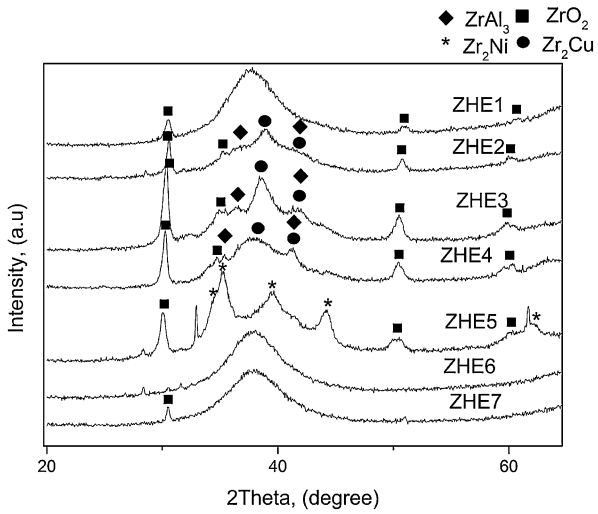

Fig. 3—XRD patterns of the alloys after annealing for 10 min at T_x temperature.

value of ΔS_{mix} is high. Lastly, the calculated weighted average melting temperature of the alloys is significantly different from the measured liquidus temperature, owing to the formation of low-temperature eutectics in the real alloys. This leads to a large difference in the Ω value for the different alloys, but is still < 1.1. Thus, according to Reference 49, these values clearly suggest that all alloys should form BMGs. But, the values are not able to indicate which alloy is a better glass former than the other(s). Therefore, we have analyzed our results in terms of the different GFA parameters described for BMGs.

As mentioned earlier, a number of different criteria were proposed to estimate/predict the GFA of alloys. These approaches achieved limited success in the sense that not all criteria could correctly predict the GFA of all the glasses studied in all the systems.[15] In spite of this, these criteria have been helpful in providing a reasonable estimate of the GFA in several instances. Table V lists the values of these different criteria for all the alloys studied in this investigation along with the values for some base alloys.

It is clear from the values listed in Table V that the ZHE3 alloy shows the highest GFA criteria/indicators (see also Figure 5) though its critical sample thickness is not high. Additionally, the alloys with the best GFA (including the base alloys) also show the largest value of the width of the supercooled liquid region (ΔT_x). However, no correlation was found between the best glass formers and the T_{rg} values. Alloys which show larger values of T_{rg} did not exhibit the best predicted GFA according to other criteria. Similarly, the GFA predicted by the criteria and the critical diameter also do not show any direct correlation. For example, ZHE2 has a critical diameter of 0.5 mm and ZHE4 1.0 mm, while ZHE6 and ZHE7 have critical diameters of 2.0 mm. In this context, it may be important to remember that several intrinsic and extrinsic parameters could actually limit the critical diameter of the fully glassy rod.[51]

Also, none of the parameters of the GFA, except for Reference 28, takes into account the width of the crystallization interval. And the ability to stabilize the supercooled liquid and to suppress the primary crystallization required for glass formation is best ensured only for the eutectic alloys. The kinetics of primary crystallization, *i.e.*, the rate of nucleation and rate of growth of nuclei of primary crystals[46,52] is very different from that of the eutectic alloys. In this connection, we can speak about the impossibility of estimating the glass-forming ability only on the basis of the entropy of the alloy and the size factor of the atoms. The parameters of the GFA should have mutual correlation only for the eutectic alloys. Therefore, it is not necessary to expect correlations with the critical diameter from alloys with different types of crystallization,[53] which is observed.

Recently, Blyskun *et al.*[24] analyzed the relationship between the critical diameter and GFA of four different Zr-based alloys and came to the conclusion that satisfying correlations were achieved between GFA and γ, γ_m, β (α), and ζ, even though they had proposed another criterion ω_m, which showed a slightly better correlation with the GFA than the other parameters. But, these authors had also shown that ΔT_x showed the weakest correlation with the GFA. There are also several other instances in the literature for such a behavior.[5]

Since the different GFA indicators are showing a good correlation with the ΔT_x values and the compositions for the best glass formers were identified, it should be possible to theoretically calculate the maximum diameter that could be expected to be fully glassy. This is possible because the authors of some of the criteria provided equations relating the critical diameter

Table III. Crystallization and Melting Enthalpies (ΔH) of the Studied Alloys (J/g)

	Peaks, Glass Crystallization				Melting	Peaks, Melt Crystallization			
	1	2	3	Total	Total	1	2	3	Total
ZHE1	11.3	6.1	7.4	24.9	− 77.3	96.7			96.7
ZHE2	12.2	1.0	12.6	25.8	− 59.1	77.6			77.6
ZHE3	14.4	1.1	11.7	27.1	− 54.8	78.1			78.1
ZHE4	4.3	13.5	14.8	32.6	− 56.0	56.5			56.5
ZHE5	10.6	1.5	4.2	16.4	− 30.8	11.6	6.9	8.6	27.2
ZHE6	6.3	1.5	13.0	20.9	− 55.5	37.4			37.4
ZHE7	4.4	4.9	18.7	28.0	− 35.1	5.0	40.8		45.9

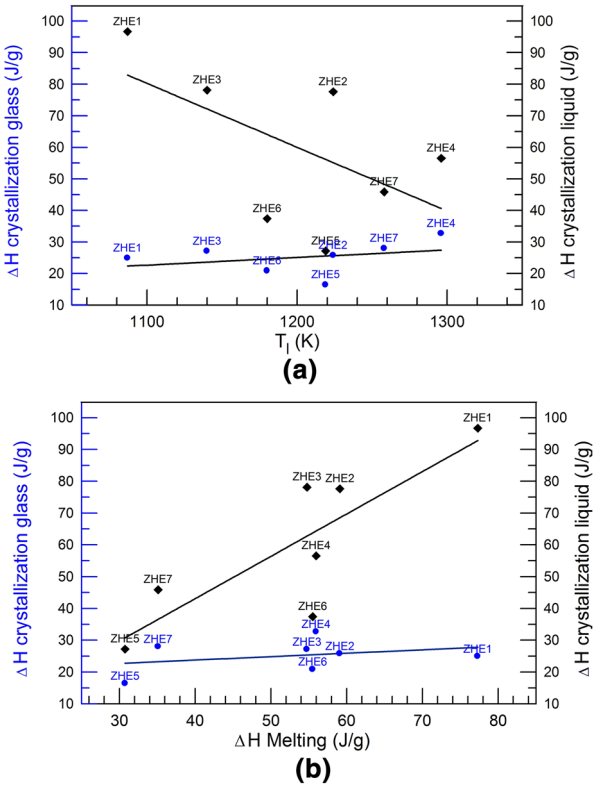

Fig. 4—Correlations (*a*) between the T_l values and the obtained enthalpies and (*b*) between the enthalpies themselves.

and the critical cooling rate to the GFA parameter. Using these equations, the values of α, β, and γ, and the critical cooling rate required to obtain 1-, 10-, and 100-mm-diameter rods are calculated and the results are presented in Table VI.[5] Interpolating the GFA parameters that were obtained for our alloys, it becomes clear that it should be possible to produce the ZHE3 alloy as a fully glassy rod with a diameter of at least 5 mm.

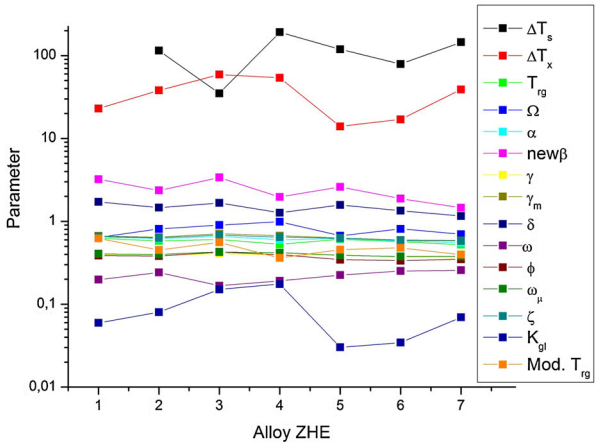

Fig. 5—Correlation of the different GFA indicators in the logarithmic scale with the alloys studied.

Table IV. Calculated Values of δ, ΔH_{mix}, ΔS_{mix}, T_m, and Ω for the Alloys Studied in this Work

Alloy	δ (Pct)	ΔH_{mix} (kJ/mol)	ΔS_{mix} (J/K/mol)	$<T_m>$ (K)	Ω
ZHE1	9.9	− 31.8	11.3	1793	0.64
ZHE2	9.9	− 27.8	12.5	1808	0.81
ZHE3	9.9	− 26.8	13.0	1847	0.90
ZHE4	9.9	− 25.7	13.8	1851	0.99
ZHE5	9.9	− 30.7	11.3	1815	0.67
ZHE6	9.9	− 25.1	11.3	1801	0.81
ZHE7	9.9	− 29.0	11.3	1797	0.70

Table V. Calculated GFA Parameters for the Different Alloys Studied in this Investigation

Alloy	D_c (mm)	T_{rg}	α	New β	γ	γ_m	δ	ω	ω_m	ϕ	ζ	Ω	K_{gl}	Modified T_{rg}
$Zr_{60}Cu_{30}Al_{10}$	8	0.58	0.65	3.09	0.41	0.72	1.56	0.16	0.43		0.69			—
$Zr_{60}Cu_{20}Ni_{10}Al_{10}$	2.5	0.72	0.72	5.62	0.42	0.80	1.94	0.11	0.47		0.75			—
ZHE1	2	0.63	0.65	3.22	0.40	0.67	1.72	0.20	0.41	0.39	0.66	0.64	0.06	0.62
ZHE2	0.5	0.58	0.62	2.36	0.39	0.64	1.46	0.24	0.40	0.38	0.63	0.81	0.08	0.45
ZHE3	0.5	0.61	0.66	3.38	0.41	0.71	1.66	0.17	0.43	0.43	0.68	0.90	0.15	0.59
ZHE4	1	0.53	0.60	1.97	0.39	0.67	1.27	0.19	0.42	0.40	0.65	0.99	0.18	0.36
ZHE5	1	0.61	0.62	2.60	0.40	0.63	1.58	0.23	0.39	0.34	0.63	0.67	0.03	0.46
ZHE6	2	0.57	0.58	1.88	0.37	0.60	1.34	0.25	0.38	0.34	0.59	0.81	0.03	0.48
ZHE7	2	0.52	0.55	1.46	0.36	0.59	1.16	0.26	0.38	0.35	0.58	0.70	0.07	0.40
Ideal value		1.0	1.0	∞	0.5	1.0	∞	0.0	0.5	0.0	1.0		∞	1

Table VI. Values of α, β, and γ and the Critical Cooling Rate (R_c) Required to Produce 1-, 10-, and 100-mm-Thick Bulk Glassy Alloy Rods

	α Parameter		β Parameter		γ Parameter	
Maximum Section thickness (mm)	α	R_c (K s^{-1})	β	R_c (K s^{-1})	γ	R_c (K s^{-1})
1	0.549	2.3×10^3	1.579	2.5×10^3	0.362	1.9×10^3
10	0.691	1	1.727	2	0.417	3
100	0.834	4.5×10^{-4}	1.876	1.3×10^{-3}	0.472	4.8×10^{-3}

IV. CONCLUSIONS

Metallic glassy samples with the nominal multicomponent composition $Zr_{50}Ti_{10}Cu_{20}Ni_{10}Al_{10}$, $Zr_{50}V_{10}Cu_{20}Ni_{10}Al_{10}$, $Zr_{50}Ti_{10}Cu_{20}Fe_{10}Al_{10}$, $Zr_{50}Ti_{10}Cu_{20}Co_{10}Al_{10}$, $Zr_{50}(Ti, V)_{10}Cu_{20}(Ni, Fe)_{10}Al_{10}$, $Zr_{50}(Ti, V, Mo, Nb)_{10}Cu_{20}(Ni, Fe)_{10}Al_{10}$, $Zr_{50}(Ti, V, Mo, Nb, Ta)_{10}Cu_{20}(Ni, Fe, Ag, Co)_{10}Al_{10}$ were produced. Partial replacement of titanium and nickel by V, Fe, Mo, Nb, Ta, Ag, and Co leads to an increased interval of the supercooled liquid region up to 59 K. Alloys with high Ti content have lower thermal stability but very low crystal growth rate. A similar effect is caused by Co addition. Although δ and Ω parameters showed that all of the multicomponent glassy alloys are in the region of BMGs, the GFA of the multicomponent alloys is not so high; likely owing to relatively large solidification interval. The main problem with finding the multicomponent alloys of high GFA is the difficulty to find the alloy composition located near the quaternary eutectic points with a small solidification interval.

ACKNOWLEDGMENTS

This work was supported by the World Premier International Research Center Initiative (WPI), MEXT, Japan and by the Ministry of Education Science of the Russian Federation in the framework of Increase Competitiveness Program of NUST«MISiS» (No. К2-2014-013 and К2-2016-071).

REFERENCES

1. W. Buckel and R. Hilsch: *Z. Phys*., 1952, vol. 132, pp. 420–22.
2. W. Buckel: *Z. Phys*., 1954, vol. 138, pp. 136–50.
3. W. Klement, R.H. Willens, and P. Duwez: *Nature*, 1960, vol. 187, pp. 869–70.
4. H.H. Liebermann: *Rapidly Solidified Alloys: Processes, Structures, Properties, Applications*, 1st ed., Marcel Dekker, New York, NY, 1993.
5. C. Suryanarayana and A. Inoue: *Bulk Metallic Glasses*, 2nd ed., CRC Press, Boca Raton, 2018.
6. C.A. Schuh, T.C. Huffnagel, and U. Ramamurty: *Acta Mater*., 2007, vol. 55, pp. 4067–4109.
7. M.W. Chen: *Annu. Rev. Mater. Res*., 2008, vol. 38, pp. 445–69.
8. C. Suryanarayana: *Mater. Today*, 2012, vol. 15, pp. 486–98.
9. T.C. Huffnagel, C.A. Schuh, and M.L. Falk: *Acta Mater*., 2016, vol. 109, pp. 375–93.
10. A. Inoue, A. Takeuchi, and T. Zhang: *Metall. Mater. Trans. A*, 1998, vol. 29A, pp. 1779–93.
11. G. Herzer: *Acta Mater*., 2013, vol. 61, pp. 718–34.
12. J.R. Scully, A. Gebert, and J.H. Payer: *J. Mater. Res*., 2007, vol. 22, pp. 302–13.
13. D.V. Louzguine-Luzgin and A. Inoue: *Handbook of Magnetic Materials*, Elsevier, New York, 2013, vol. 21, pp. 131–71.
14. N. Nishiyama, K. Takenaka, H. Miura, N. Saidoh, Y. Zeng, and A. Inoue: *Intermetallics*, 2012, vol. 30, pp. 19–24.
15. C. Suryanarayana, I. Seki, and A. Inoue: *J. Non-Cryst. Solids*, 2009, vol. 355, pp. 355–60.
16. D. Turnbull: *Contemp. Phys*., 1969, vol. 10, pp. 473–88.
17. A. Inoue: *Mater. Trans. JIM*, 1995, vol. 36, pp. 866–75.
18. K. Mondal and B.S. Murty: *J. Non-Cryst. Solids*, 2005, vol. 351, pp. 1366–71.
19. Z.Z. Yuan, S.L. Bao, Y. Lu, D.P. Zhang, and L. Yao: *J. Alloy. Compd*., 2008, vol. 459, pp. 251–60.
20. Z.P. Lu and C.T. Liu: *Acta Mater*., 2002, vol. 50, pp. 3501–12.
21. X.H. Du, J.C. Huang, C.T. Liu, and Z.P. Lu: *J. Appl. Phys*., 2007, vol. 101, pp. 086108-1–086108-3.
22. Q.J. Chen, J. Shen, D. Zhang, H.B. Fan, J.F. Sun, and D.G. McCartney: *Mater. Sci. Eng. A*, 2006, vol. 433, pp. 155–60.
23. Z.L. Long, H.Q. Wei, Y.H. Ding, P. Zhang, G.Q. Xie, and A. Inoue: *J. Alloy. Compd*., 2009, vol. 475, pp. 207–19.
24. P. Blyskun, P. Maj, M. Kowalczyk, J. Latuch, and T. Kulik: *J. Alloy. Compd*., 2015, vol. 625, pp. 13–17.
25. G.J. Fan, H. Choo, and P.K. Liaw: *J. Non-Cryst. Solids*, 2007, vol. 353, pp. 102–107.
26. X.H. Du and J.C. Huang: *Chin. Phys. B*, 2008, vol. 17, pp. 249–54.
27. A. Hrubý: *Czech. J. Phys*., 1972, vol. B22, pp. 1187–93.
28. N. Nishiyama and A. Inoue: *Mater. Trans*., 2008, vol. 43, pp. 1913–17.
29. Z.P. Lu and C.T. Liu: *J. Mater. Sci*., 2004, vol. 39, pp. 3965–74.
30. W.H. Wang: *Prog. Mater. Sci*., 2007, vol. 52, pp. 540–96.
31. D.V. Louzguine-Luzgin, N. Chen, A.Yu. Churymov, L.V. Louzguina-Luzgina, V.I. Polkin, L. Battezzati, and A.R. Yavari: *J. Mater. Sci*., 2015, vol. 50, pp. 1783–93.
32. A. Inoue, T. Zhang, and T. Masumoto: *Mater. Trans., JIM*, 1990, vol. 31, pp. 177–83.
33. D.V. Louzguine-Luzgin, S.V. Ketov, Z. Wang, M.J. Miyama, A.A. Tsarkov, and A.Yu. Churyumov: *Mater. Sci. Eng. A*, 2014, vol. 616, pp. 288–96.
34. R. Ray, B.C. Giessen, and N.J. Grant: *Scripta Metall*., 1968, vol. 2, pp. 357–59.
35. Q.S. Zhang, W. Zhang, and A. Inoue: *Mater. Trans*., 2007, vol. 48, pp. 3031–33.
36. H.B. Lou, X.D. Wang, F. Xu, S.Q. Ding, Q.P. Cao, K. Hono, and J.Z. Jiang: *Appl. Phys. Lett*., 2011, vol. 99, p. 051910.
37. J. Eckert, J. Das, K.B. Kim, F. Baier, M.B. Tang, W.H. Wang, and Z.F. Zhang: *Intermetallics*, 2006, vol. 14, pp. 876–81.
38. Y. Yokoyama, T. Yamasaki, P.K. Liaw, and A. Inoue: *Acta Mater*., 2008, vol. 56, pp. 6097–6108.
39. Q.S. Zhang, W. Zhang, D.V. Louzguine-Luzgin, and A. Inoue: *Mater. Sci. Forum*, 2010, vols. 654–656, pp. 1042–45.
40. T.H. Kim, A.K. Gangopadhyay, L.Q. Xing, G.W. Lee, Y.T. Shen, K.F. Kelton, A.I. Goldman, R.W. Hyers, and J.R. Rogers: *Appl. Phys. Lett*., 2005, vol. 87, p. 251924.
41. B.S. Murty, J.W. Yeh, and S. Ranganathan: *High Entropy Alloys*, Butterworth-Heinemann, London, 2014.
42. M.C. Gao, J.-W. Yeh, P.K. Liaw, and Y. Zhang: *High Entropy Alloys: Fundamentals and Applications*, Springer, New York, 2016.
43. B. Cantor: *Entropy*, 2014, vol. 16, pp. 4749–68.

44. L. Ma, L. Wang, T. Zhang, and A. Inoue: *Mater. Trans.*, 2002, vol. 43, pp. 277–80.
45. A. Inoue, Z. Wang, D.V. Louzguine-Luzgin, Y. Han, F.L. Kong, E. Shalaan, and F. Al-Marzouki: *J. Alloy. Compd.*, 2015, vol. 638, pp. 197–203.
46. D.V. Louzguine-Luzgin, G. Xie, W. Zhang, and A. Inoue: *Mater. Sci. Eng. A*, 2007, vol. A465, pp. 146–52.
47. D.V. Louzguine and A. Inoue: *J. Mater. Res.*, 2002, vol. 17, pp. 2112–20.
48. Y. Zhang, Y.J. Zhou, J.P. Lin, G.L. Chen, and P.K. Liaw: *Adv. Eng. Mater.*, 2008, vol. 10, pp. 534–38.
49. X. Yang and Y. Zhang: *Mater. Chem. Phys.*, 2012, vol. 132, pp. 233–38.
50. I.A. Tomilin and S.D. Kaloshkin: *Mater. Sci. Technol.*, 2015, vol. 31, pp. 1231–34.
51. D.V. Louzguine-Luzgin, D.B. Miracle, and A. Inoue: *Adv. Eng. Mater.*, 2008, vol. 10, pp. 1008–15.
52. A.S. Aronin, G.E. Abrosimova, A.F. Gurov, Yu.V. Kir'yanov, and V.V. Molokanov: *Mater. Sci. Eng. A*, 2001, vol. 304–306, pp. 375–79.
53. R.V. Sundeev, A.M. Glezer, and A.V. Shalimova: *Mater. Lett.*, 2016, vol. 175, pp. 72–74.